



Measurement of $\sigma(\text{p}\bar{\text{p}} \rightarrow \text{Z}) \cdot \text{Br}(\text{Z} \rightarrow \tau^+\tau^-)$ with 1 fb^{-1} at $\sqrt{s} = 1.96 \text{ TeV}$

The DØ Collaboration
URL <http://www-d0.fnal.gov>
(Dated: August 11, 2007)

We measure the cross section for Z production times the branching fraction to tau lepton pairs $\sigma \cdot \text{Br}(\text{Z} \rightarrow \tau^+\tau^-)$ in $\text{p}\bar{\text{p}}$ collisions at $\sqrt{s} = 1.96 \text{ TeV}$. The measurement was performed in the channel in which one tau lepton decays into $\mu\nu_\mu\nu_\tau$, and the other into hadrons + ν_τ or $e\nu_e\nu_\tau$. The data sample corresponds to an integrated luminosity of 1.0 fb^{-1} collected with the DØ detector at the Fermilab Tevatron between September 2002 and February 2006. The final sample contains 1527 candidate events with an estimated 20% background from misidentified tau leptons. We obtain $\sigma \cdot \text{Br} = 247 \pm 8 \text{ (stat.)} \pm 13 \text{ (sys.)} \pm 15 \text{ (lum.) pb}$, which is consistent with the standard model prediction.

I. INTRODUCTION

We describe a measurement of $\sigma \cdot \text{Br}(Z \rightarrow \tau^+ \tau^-)$ in $p\bar{p}$ collisions at $\sqrt{s} = 1.96$ TeV based on an event sample containing a single isolated muon assumed to come from a tau lepton decay and a tau candidate reconstructed as a narrow jet that could be produced by a tau lepton decaying hadronically or into an electron and neutrinos. This measurement is of interest not only as a useful test of our ability to identify tau leptons but also because any excess over the expected $\sigma \cdot \text{Br}$ could be an indication of a source other than Z bosons for $\mu\tau$ pair events [1]. The precision of this result is significantly improved compared to the earlier publication by the DØ collaboration [2].

II. DATA AND MONTE CARLO SAMPLES

This analysis is based on the data collected between September 2002 and February 2006 by the DØ experiment (the whole Run IIa data set), corresponding to an integrated luminosity of (1003 ± 61) pb^{-1} [3]. Only events in which all detectors were in good working condition were considered. A single muon trigger requiring hits in the muon system in combination with a high p_T track reconstructed in the central tracking system was required to have fired in each event. The trigger efficiency was computed using a control data sample of $Z \rightarrow \mu^+ \mu^-$ events and was determined to be $(50.2 \pm 1.8)\%$.

The contribution of the majority of backgrounds as well as the efficiency of the selection for signal $Z \rightarrow \tau^+ \tau^-$ events were estimated using Monte Carlo (MC) simulations. All simulated samples were generated with PYTHIA [4] (version 6.323) using the CTEQ6.1L PDF set. Simulation of the DØ detector was done using GEANT3 [5]. The code used for the reconstruction of simulated events is equivalent to the one used for data. Noise in the detector and the contribution to the event coming from other simultaneous interactions were simulated using zero bias events coming from data. To take into account the luminosity dependence of the underlying event, each MC event was given a weight equal to the ratio of data to MC normalized numbers of events in the bin of instantaneous luminosity of the zero bias event used as overlay in that particular MC event.

Corrections were applied to all the MC to obtain overall good agreement between simulation and collider data. The momentum scale and resolution for muons in the MC were tuned to reproduce the Z boson invariant mass distribution observed in data. The MC jets were smeared in energy using a random Gaussian distribution to match the resolutions observed in data for different regions of the detector. The p_T spectrum of the Z boson for events generated with PYTHIA is known to have a different shape compared to the one measured in data [6]. Therefore the p_T of the Z boson was reweighted with a modified Fermi function obtained from fitting of the ratio of the differential Z boson cross sections as a function of Z boson p_T measured in data to the one obtained from Monte Carlo simulation. Small differences in acceptance between data and simulation were found to be due to the beam shape modelling in MC. A correction factor was used to account for the decrease in acceptance measured in $Z \rightarrow \mu^+ \mu^-$ events after reweighting the simulated z position of the primary vertex such that it reproduced the distribution observed in data.

Efficiencies for a muon or a track to be reconstructed both in data and MC were calculated using control samples of $Z \rightarrow \mu^+ \mu^-$ events. Efficiency correction factors for MC events as a function of different muon position parameters were applied accordingly. The samples are normalized to the expected number of events evaluated using the luminosity of the data sample and the theoretical values of the NNLO cross sections in the case of Z and W production [7] or NLO cross sections for all other processes where the NNLO calculation is not available [8].

III. IDENTIFICATION OF MUONS AND TAU CANDIDATES

Muons are identified based on their signature in the three layer muon detector system, which has a toroid magnet placed between the first and second layers. The track reconstructed from the hits in the muon layers is required to match a track from the central tracking detectors for which the distance of closest approach with respect to the primary vertex of the event in the (x, y) plane is less than 0.2 cm and the fit of the hits has $\chi^2/\text{d.o.f.} < 4$. The momentum of the muons was measured exclusively by the central tracking detectors.

A tau candidate is a collection of: a calorimeter cluster reconstructed using the simple cone algorithm, tracks associated to the calorimeter cluster of which at least one has $p_T > 1.5$ GeV, but with a total invariant mass less than 1.8 GeV, and electromagnetic (EM) sub-clusters reconstructed using a nearest neighbor algorithm seeded in the finely segmented third layer of the calorimeter. The size of the cone used for the reconstruction of the calorimeter cluster is $R = 0.5$, where $R = \sqrt{(\Delta\phi)^2 + (\Delta\eta)^2}$, $\Delta\phi$ is the difference in azimuthal angle and $\Delta\eta$ the difference in pseudorapidity between the axis of symmetry of the cone and each of the calorimeter towers. Isolation variables are calculated using a cone of $R = 0.3$ within which most of the activity must be identified. The tracks associated to the tau candidate must also be contained within this cone.

Tau candidates are classified as type 1, 2 or 3, depending on the number of tracks and EM clusters they possess. Type 1 tau candidates have exactly one associated track and no EM sub-clusters, type 2 have one associated track but in addition one or more EM sub-clusters, and type 3 have at least two associated tracks. These categories correspond roughly to pure one-prong decays, one-prong plus neutral decays (as well as electrons, which were treated as type 2 tau candidates in this analysis) and three prong decays of the tau.

Due to the large number of jets reconstructed as tau candidates, additional selection criteria had to be applied in order to distinguish the true tau leptons from jets. Three neural networks (NN), one for each tau type, were trained using $Z \rightarrow \tau^+ \tau^-$ Monte Carlo events as signal and events with a jet back-to-back to a non-isolated muon from data as background. The NNs used isolation variables based on tracks, hadronic and EM calorimeter clusters, as well as shower shape variables and correlation variables between calorimeter and tracks. Figure 1 shows the discrimination obtained using the NNs. Requiring that the NN output is larger than 0.9 results for all three types in a background rejection of almost a factor of 50. This reduces the probability for a jet to be misidentified as a tau lepton to 1.1% for the sum of all types (from 52% without the NN output requirement) while maintaining a total efficiency of close to 70% for real tau leptons which decay hadronically or to an electron and neutrinos. For a complete description of the neural networks and details on their performance on data and Monte Carlo see Ref. [9].

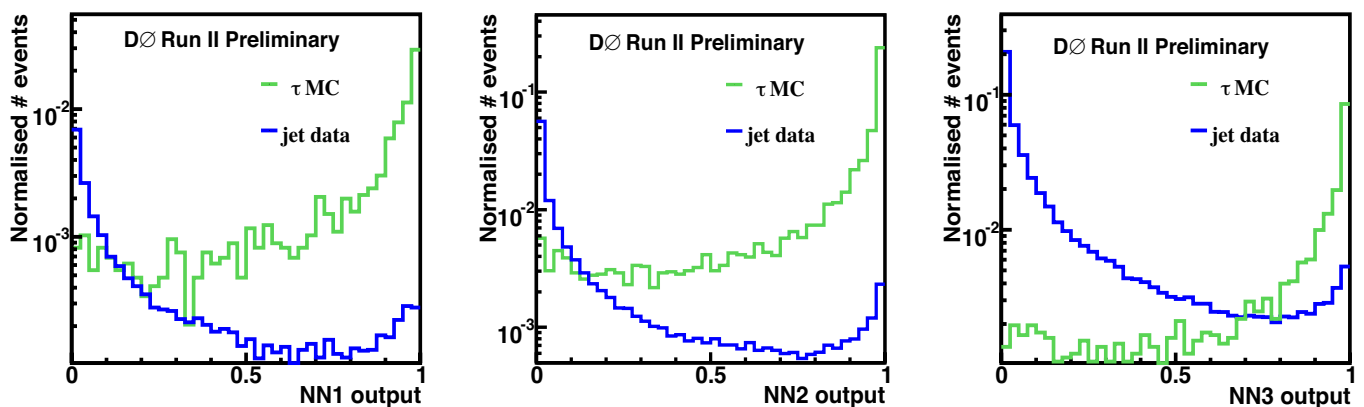


FIG. 1: NN output distributions for type 1 (left), type 2 (middle) and type 3 (right) tau candidates. The ratio of signal to background is arbitrary, but the relative amounts of type 1, type 2 and type 3 events in background and signal are not. The distributions are normalized with respect to each other such that the sum over the three types is 1 for both signal and background.

IV. ENERGY CORRECTION FOR TAU CANDIDATES

To compare the visible invariant mass of the tau pairs between data and Monte Carlo, it is important to obtain a correct energy scale for the tau candidate, notably in the case of a hadronically decaying tau lepton.

For the type 1 tau candidates, the $p_{(T)}$ of the track was used as the best estimate of the (transverse) energy of the tau, for the energy region where the tracking resolution is superior to the calorimeter energy resolution (up to calorimeter cluster energy of 70 GeV). The method which proved to be most successful for the types 2 and 3 tau candidates was the one in which the (transverse) energy of the tau was estimated using:

$$E_{(T)}^{corr} = \sum p_{(T)}^{trk} + E_{(T)}^{cal} - \sum R(p_{(T)}^{trk}, \eta) \cdot p_{(T)}^{trk}, \quad (1)$$

where $p_{(T)}^{trk}$ is the $p_{(T)}$ of tracks associated to the τ , $E_{(T)}^{cal}$ is the (transverse) energy deposited by the tau in the calorimeter and $R(p_{(T)}^{trk}, \eta)$ is a number typically between 0.6 and 0.9 representing the response of the calorimeter to π^\pm as a function of the energy and rapidity of the π^\pm . As the resolution of the calorimeter becomes better than the tracking resolution for calorimeter cluster energies higher than 70 GeV (type 1), 100 GeV (type 2) or 120 GeV (type 3), the energy of the calorimeter cluster was used in that region, after applying η and energy dependent scale factors obtained from Monte Carlo.

Since the charged pion response in data is not perfectly reproduced in Monte Carlo, we used events in which GEISHA [10], the default code used for the simulation of hadronic interactions, was replaced by gCALOR [11] for

a more precise simulation of the single charged pion interactions. The charged pion response obtained using these special simulations resulted in a good description of the data. The neutral energy measurement, mostly important for type 2 taus, is dominated by electromagnetic showers in the calorimeter. Electromagnetic shower simulation in the Monte Carlo describes the data response sufficiently well for the scope of this analysis, therefore no corrections related to the neutral pion response were applied.

V. MISSING E_T RECONSTRUCTION AND CORRECTION

The raw missing transverse energy (\cancel{E}_T) is defined as the vector equal in length and opposite in direction to the vectorial sum of transverse energies of the calorimeter cells. A correction algorithm is applied to suppress contributions from noise. The transverse momenta of muons are subtracted from this vector, after corrections for the energy deposited by the muons in the calorimeter have been applied. When the tau candidate matched a reconstructed electron the normal $D\bar{O}$ energy corrections were applied. For other jets corresponding to tau candidates, the tau energy corrections from the previous section were applied.

VI. EVENT SELECTION

The preselection required one isolated muon reconstructed within $|\eta_{\text{det}}| < 1.6$ using a number of hits in the muon detector to be matched to a good quality central track. The transverse momentum of the muon as measured by the central tracking detectors satisfied $p_T^\mu > 15$ GeV. No other muon matched to a central track with $p_T > 10$ GeV was allowed to be present in the event. Quantitatively, the muon isolation required the sum of energies of all cells situated in a hollow cone around the direction of the tagged muon with $0.1 < R < 0.4$, as well as the sum of all tracks in a cone of $R < 0.5$, excluding the muon track, to be less than 2.5 GeV.

The preselection further required one tau candidate with $p_T > 15$ GeV, $|\eta| < 2$, scalar sum of the transverse momenta of all tracks associated to the tau candidate > 15 GeV for types 1 and 3 and > 5 GeV for type 2 tau candidates, $NN > 0.3$ and no other muon matching the tau candidate. Type 3 tau candidates with 2 tracks were only considered if both tracks had the same charge. The tau candidate was required to have a charge opposite to that of the muon and the distances in the z direction between the muon and the primary vertex, the tau candidate and the primary vertex, as well as the distance between the muon and the tau candidate had to be less than 1 cm.

In total 8426 events passed these criteria. To reduce the W +jets as well as the $Z \rightarrow \mu^+\mu^-$ backgrounds, another selection criterion was used, based on a variable which gives an approximation of the W mass, called \hat{M}_W :

$$\hat{M}_W = \sqrt{2E^\nu E^\mu (1 - \cos \Delta\phi)}, \quad (2)$$

where E^ν is an approximation of the neutrino energy calculated using the transverse momentum of the muon p_T^μ , the energy of the muon E^μ and the missing transverse energy \cancel{E}_T , given by:

$$E^\nu = \cancel{E}_T E^\mu / p_T^\mu \quad (3)$$

and $\Delta\phi$ is the angle between the missing E_T and the muon in the $r\phi$ plane.

For the final selection the lower limit on the NN output for the tau candidates was raised to 0.9 for types 1 and 2, and to 0.95 for type 3 tau candidates. The final selection also required $\hat{M}_W < 20$ GeV. A total of 1527 events passed all the selection criteria in the data sample.

VII. BACKGROUND

The dominant background is from multijet (QCD) processes, mainly from $b\bar{b}$ events where the muon isolation requirement is met and one of the jets satisfies the tau candidate selection criteria. Another significant source of events with isolated muons and tau candidates from misidentified jets is W + jets production, where the W boson decays into a muon and a neutrino. The $Z \rightarrow \mu^+\mu^-$ background is reduced by the requirement that no other loose muon should be found in the event. However, a small number of events will still be selected when one of the muons is not identified. Small contributions are also expected from $W \rightarrow \tau\nu$ and $WW \rightarrow l\nu l\nu$, as well as $t\bar{t}$ production. The contributions from WZ and ZZ events were estimated to yield below one event each after the final selection criteria were applied and are therefore considered negligible in this analysis. All backgrounds, except that from QCD, were estimated using MC simulations.

The QCD background is estimated using the events that satisfy all requirements placed on the signal sample except that the muon and tau candidate have the same charge. We will call this the same-sign (SS) sample. To test the assumption that the number of SS events is equal to the number of opposite-sign (OS) background events, a special data sample was selected, named ‘‘QCD sample’’ from here on, in which the events passed all other requirements placed on the signal sample, but failed the isolation criteria and the cut on the tau NN output. Instead of the isolation requirement used for the signal events, the events in the QCD sample had the sum of energies of all cells inside a hollow cone around the direction of the muon between $R = 0.1$ and $R = 0.4$ in the range 2.5 to 10 GeV, and the sum of the momenta of all tracks, excluding the muon track, in the cone of $R < 0.5$ around the muon direction in the same interval (2.5 – 10 GeV). To avoid the contribution from $Z \rightarrow \tau^+\tau^-$ signal events, an upper limit on the tau NN output was placed at 0.8. The muon p_T was required to be at least 10 GeV instead of 15 GeV, to increase the statistics of this sample. The QCD sample is expected to be completely dominated by multijet processes, but may also include events in which a W decaying into a muon was produced in association with a jet. The W+jet contribution was reduced by placing a limit on the azimuthal angle between the muon and the tau and requiring that they are back to back ($|\phi_\mu - \phi_\tau| > 2.5$ rad). A slight excess of OS events was observed in the QCD sample. No significant dependence of the OS/SS ratio as a function of p_T and NN output was observed for the three types of tau candidates in the QCD sample. Correction factors (f_i) 1.13 ± 0.03 , 1.08 ± 0.01 and 1.06 ± 0.01 for each tau type were obtained. The number of events in the SS sample is corrected for the contribution from $Z \rightarrow \mu^+\mu^-$, $Z \rightarrow \tau^+\tau^-$ and $W \rightarrow \tau\nu$ obtained from MC, with a total of 3 events for type 1, 8 for type 2 and 12 for type 3 tau candidates after all cuts. The more substantial contribution from $W \rightarrow \mu\nu$ events is accounted for separately.

A part of the W+jets background has already been included in the SS sample which is used as an estimate of the QCD background. However, we do expect a significant excess of OS events compared to the number of SS events due to the fact that a high percentage of W+1 jet events come from quark jets. The number of W+jets events in data was estimated by selecting a sample that is expected to have a large contribution from that channel and low or negligible contributions from Z boson production. Such a W+jets enriched sample can be obtained by requiring an isolated muon with $p_T > 20$ GeV, a tau candidate with $0.3 < NN < 0.8$, $|\phi_\mu - \phi_\tau| < 2.7$ rad and $\hat{M}_W > 40$ GeV. We can expect that mostly QCD and W+jets events will contribute to this sample. Using the fact that we expect an excess of OS events compared to SS of $(7 \pm 3)\%$ for QCD (averaged over all types) and $(60 \pm 40)\%$ for $W \rightarrow \mu\nu$ (estimated from data, in the sample with the cuts listed above, but requiring a tighter cut $\hat{M}_W > 60$ GeV), we can calculate the number of W + jets events in the W + jets enriched data sample by solving the following system of two equations:

$$N_W + N_{QCD} = N_{OS} + N_{SS} = 3243 \quad (4)$$

$$0.6 \cdot N_W + 0.07 \cdot N_{QCD} = N_{OS} - N_{SS} = 989 \quad (5)$$

which gives $N_W = 1438 \pm 567$. The number of expected W+jets for this sample, estimated using MC normalized to the NNLO cross section and the luminosity from data, is 2152 ± 47 (56/19 OS/SS events for type 1, 319/85 OS/SS events for type 2 and 1102/571 OS/SS events for type 3). The ratio between the number of events calculated for data by solving the above system of equations and the one expected from MC will be used as a normalization factor for this background in the signal region. The error on N_W from data is taken as a systematic error. The estimated number of W + jets events in the signal sample, not considering the ones already included in the SS sample, is 14 ± 6 .

VIII. ESTIMATING THE $Z \rightarrow \tau^+\tau^-$ SIGNAL

Several distributions were compared between the data and the predicted sum of background and $Z \rightarrow \tau^+\tau^-$ for the SM cross section and branching ratio. All these distributions show good agreement after each of the pre-selection, NN selection and anti-W requirement stages.

The signal is best characterized by the visible mass distribution, where visible mass is defined as:

$$\text{Visible Mass} = \sqrt{(P_\mu + P_\tau + \cancel{P}_T)^2}, \quad (6)$$

with $P_{\mu,\tau} = (E_{\mu,\tau}, P_{\mu,\tau}^x, P_{\mu,\tau}^y, P_{\mu,\tau}^z)$ and $\cancel{P}_T = (\cancel{E}_T, \cancel{P}_T^x, \cancel{P}_T^y, 0)$. In Fig. 2 the visible mass distribution is shown for each of the tau types and for the sum of all types, for events which pass the final selection requirements. In Fig. 3 the distribution for the sum of all types is shown on a logarithmic scale. Reasonable agreement can be observed between the data and the sum of the background SM processes and $Z \rightarrow \tau^+\tau^-$ signal, using the SM predicted cross section for the latter [7].

Table I shows the number of events expected for each tau type from each of the backgrounds, as well as from $Z \rightarrow \tau^+\tau^-$ signal normalized with the NNLO cross section [7]. It also shows the total number of expected background

and signal events in comparison to the number of events observed in data, for the three levels of selection mentioned above: preselection, preselection + NN output > 0.9 (0.95 for type 3 tau candidates) and after all selection criteria were applied. Good agreement was observed between the predicted and observed numbers of events at each level of selection for all tau types.

It is estimated from MC that a fraction of $5.3 \cdot 10^{-3}$ of all $Z \rightarrow \tau^+\tau^-$ events will get a wrong sign for either the muon or the tau candidate, therefore appearing as SS events. From the number of $Z \rightarrow \tau^+\tau^-$ events obtained from subtracting the estimated background from the number of events in the final sample, we calculate the number of $Z \rightarrow \tau^+\tau^-$ events reconstructed as SS to be 8.2. Assuming that the probability of sign flipping is the same for going from OS to SS as it is the other way around, and given that the estimated background in the final sample is 20%, we estimate that a number of 7 events should be added to the number of events in the OS sample when calculating the $Z \rightarrow \tau^+\tau^-$ cross section, as a second order correction.

Reconstructing a second track close to a first reconstructed track was found to be more efficient in MC compared to data. A correction factor of 0.97 ± 0.02 (obtained by comparing the number of type 3 tau candidates with 2 and 3 tracks in data and MC and taking into account that there are twice as many SS as OS combinations when one of the three tracks is lost) was applied to the simulated events containing type 3 tau candidates.

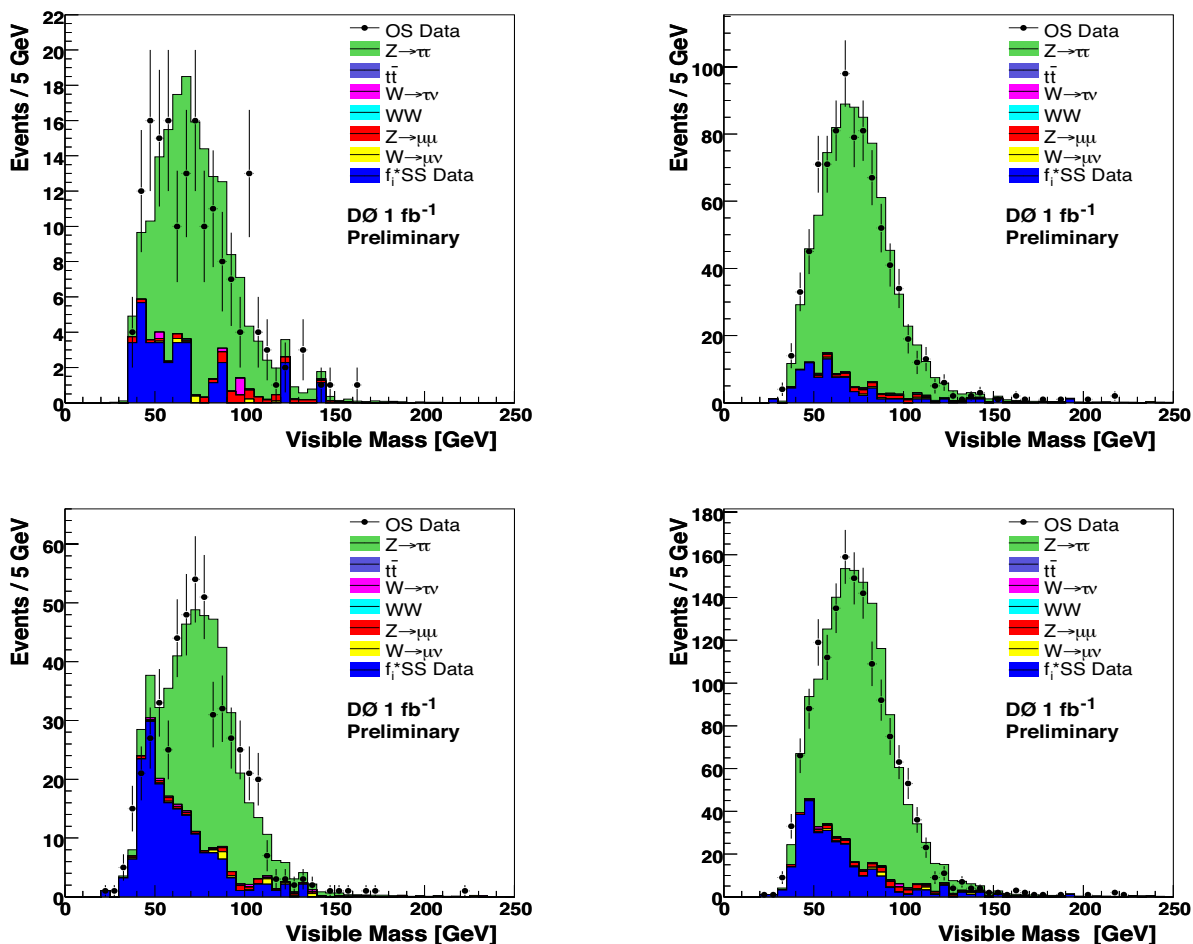


FIG. 2: Visible mass distribution for type 1 tau events (upper left), type 2 tau events (upper right), type 3 tau events (lower left) and the sum of the three tau types (lower right). The data are the points with error bars. The different components of the SM expectation are as given in the legend. The $Z \rightarrow \tau^+\tau^-$ signal is normalized to the theoretical expectation calculated at NNLO using MRST2004 parton distribution functions [7].

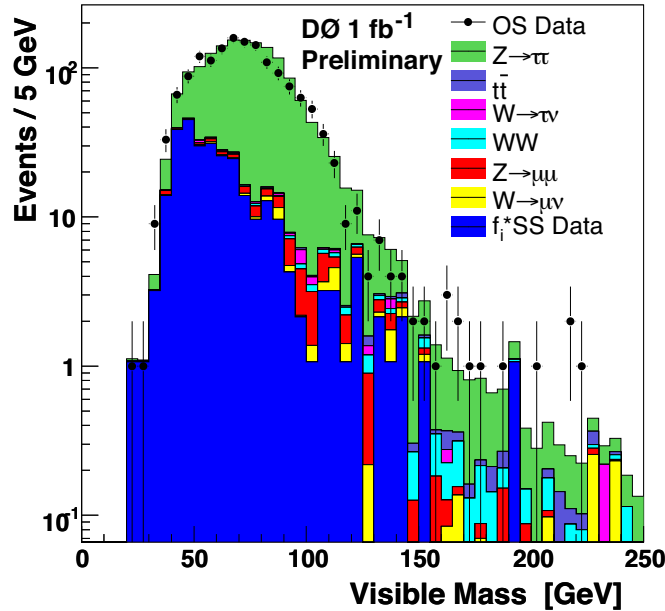


FIG. 3: Visible mass distribution for all tau types on logarithmic scale. The data are the points with error bars. The different components of the SM expectation are as given in the legend. The $Z \rightarrow \tau^+\tau^-$ signal is normalized to the theoretical expectation calculated at NNLO using MRST2004 parton distribution functions [7].

Process	type 1			type 2			type 3		
	Preselection	Preselection + NN > 0.9	all cuts	Preselection	Preselection + NN > 0.9	all cuts	Preselection	Preselection + NN > 0.95	all cuts
$Z \rightarrow \tau^+\tau^-$	297 ± 4	224 ± 4	141 ± 3	1440 ± 9	1108 ± 8	754 ± 7	680 ± 6	468 ± 5	344 ± 5
tt	2.7 ± 0.3	2 ± 0.3	0.2 ± 0.1	32 ± 1	27 ± 1	2.4 ± 0.3	28 ± 1	4 ± 0.4	0.5 ± 0.1
$W \rightarrow \tau\nu$	10 ± 2	4 ± 1	1.5 ± 0.8	48 ± 4	14 ± 2.2	1.4 ± 0.7	162 ± 7	21 ± 2.7	3.7 ± 1.2
WW	7 ± 0.3	6 ± 0.3	0.4 ± 0.1	77 ± 1	72 ± 1	6.7 ± 0.3	9 ± 0.4	6 ± 0.5	0.5 ± 0.1
$Z \rightarrow \mu^+\mu^-$	56 ± 2	42 ± 1.5	6 ± 0.6	169 ± 3	105 ± 3	13 ± 0.8	178 ± 3	37 ± 1	9 ± 0.7
$W \rightarrow \mu\nu$	106 ± 11	35 ± 5	1.8 ± 1.2	427 ± 18	105 ± 9	6 ± 2	1427 ± 32	207 ± 13	14 ± 3.5
QCD	215 ± 15	54 ± 8	28 ± 5.5	599 ± 25	143 ± 12	71 ± 9	2290 ± 47	302 ± 18	152 ± 13
Predicted	694 ± 18	367 ± 11	179 ± 7	2792 ± 32	1574 ± 18	854 ± 12	4774 ± 59	1045 ± 23	524 ± 15
Data	726	380	172	2863	1548	847	4837	1004	508

TABLE I: Number of events expected for each tau type from each of the backgrounds, as well as from $Z \rightarrow \tau^+\tau^-$ signal normalized with the NNLO cross section, the sum of background and signal and the number of events observed in data, for three levels of cuts: preselection, preselection + NN output > 0.9 (0.95 for type 3) and after all selection criteria were applied

IX. SYSTEMATIC UNCERTAINTIES

Systematic uncertainties on background estimates are derived from the errors quoted for each estimate in section VII.

The systematic uncertainty related to the tau energy measurement was estimated by scaling the charged pion response used for data by the largest difference found between the response measured in data and the response obtained using gCALOR (7%) and recalculating the acceptance applying all cuts. The value of the uncertainty on the cross section due to the uncertainty on the charged pion response was found to be 1%. NN systematic uncertainties were calculated using statistical ensembles of events in which each input variable was allowed to fluctuate within the difference observed between the distributions of that particular variable in data and MC. The RMS of the ratio of the number of events passing a certain NN cut to the number of events in the ensembles, called ensemble cut ratio, was taken as a measure of the uncertainty. The RMS of the ensemble cut ratio distributions obtained by varying each input variable were then summed quadratically and the square root of the sum was taken as the overall systematic uncertainty. The estimated uncertainties were 3.8% for type 1, 1.2% for type 2 and 3.7% for type 3 tau candidates.

The uncertainty due to the tau candidate track reconstruction efficiency is taken to be the same as the uncertainty on reconstructing muon tracks with the same quality requirements and was estimated using $Z \rightarrow \mu^+ \mu^-$ events. The value of this uncertainty is 1.4%. The uncertainty on the correction factor due to differences between data and MC in tracking efficiency for type 3 taus is added in quadrature to this value, resulting in a total uncertainty related to the tau tracks of 1.5%. The systematic uncertainties due to muon identification and muon track matching were determined to be 0.5% and 0.8%, respectively. The systematic uncertainty due to the reweighting of the Z boson p_T distribution is 1.6%. The uncertainty on trigger efficiency amounts to 3.6% and was estimated taking into account a variety of effects such as the bias related to the choice of the control sample, the variation with an additional cut and background contamination, variations in time or due to increasing luminosity, the choice of binning and the choice of parameters for the efficiency, as well as the limited statistics. The uncertainty on the total integrated luminosity is 6.1%, and the PDF error was determined to be 1.7%. Table II summarizes all the systematic uncertainties.

Source	Value
Tau Energy Scale	1.0 %
NN	2.4 %
Tau track reconstruction	1.5 %
QCD background	0.7 %
$W \rightarrow \mu\nu$ background	0.5 %
Trigger	3.6 %
Muon track match	0.8 %
Muon identification	0.4 %
Z p_T reweighting	1.6 %
PDF	1.7 %
Total (except Luminosity)	5.4 %
Luminosity	6.1 %

TABLE II: Systematic uncertainties on $\sigma \cdot \text{BR}(Z/\gamma^* \rightarrow \tau^+ \tau^-)$

X. RESULTS AND DISCUSSION

The cross section times branching ratio for $p\bar{p} \rightarrow Z/\gamma^* \rightarrow \tau^+ \tau^-$ is given by the number of signal events divided by the product of the total efficiency and the integrated luminosity. The number of signal events estimated from Table I, with the second order correction for signal events reconstructed as SS, is 1216. Since Table I shows the estimated number of events from the Z boson mass range 15 – 500 GeV, other corrections have to be made in order to compare the result of this analysis with theoretical cross sections. To limit the mass range to 60 – 130 GeV, the number of events expected from the mass region 15 – 60 GeV (7 events) as well as from the 130 – 500 GeV mass region (27 events) were subtracted from the number of signal events in data. The total efficiency for $Z \rightarrow \tau^+ \tau^-$ events in the 60 – 130 GeV mass region is $4.7 \cdot 10^{-3}$, which also includes the trigger efficiency of 50.2 %. Finally, a factor of 0.98 [13] was applied to estimate the pure Z cross section as opposed to the Z/γ^* cross section for this mass region. Given the systematic uncertainties listed in Table II and an integrated luminosity of 1003 pb^{-1} , we estimate

$$\sigma(p\bar{p} \rightarrow Z) \cdot \text{BR}(Z \rightarrow \tau^+ \tau^-) = 247 \pm 8 \text{ (stat)} \pm 13 \text{ (sys)} \pm 15 \text{ (lumi)} \text{ pb},$$

which is in good agreement with the standard model NNLO prediction of $251.9_{-11.8}^{+5.0}$ pb [7] that results from the NNLO calculation using the MRST2004 parton density functions, as well as with the $241.6_{-3.2}^{+3.6}$ pb [12] value obtained at NNLO using CTEQ6.1M PDF parametrization. Figure 4 shows a comparison of this result with other Z cross section measurements, as well as with the theoretical calculation from [7]. We therefore convincingly demonstrate the DØ experiment’s ability to identify and reconstruct tau leptons and thus experimentally establish our sensitivity for observing signatures such as $H \rightarrow \tau^+ \tau^-$.

Acknowledgments

We thank the staffs at Fermilab and collaborating institutions, and acknowledge support from the Department of Energy and National Science Foundation (USA), Commissariat à L’Energie Atomique and CNRS/Institut National de Physique Nucléaire et de Physique des Particules (France), Ministry for Science and Technology and Ministry for

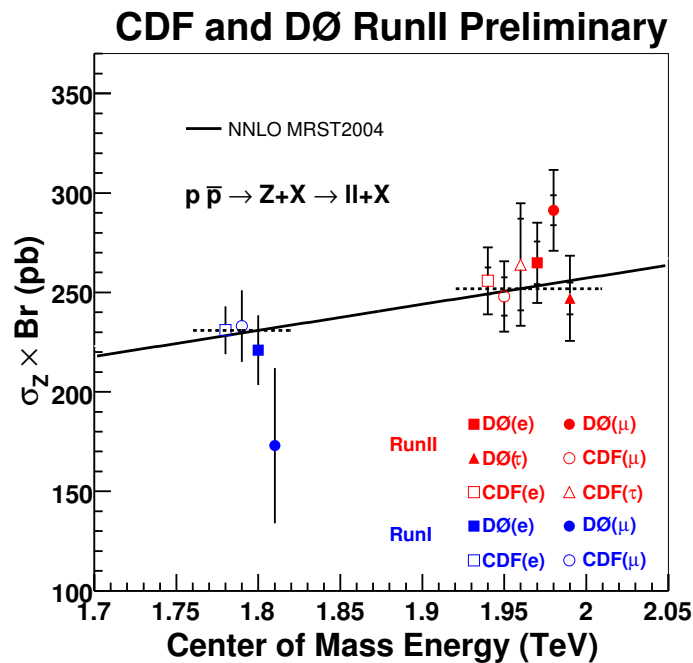


FIG. 4: Comparison of the available measured Z cross section times branching ratios performed by $D\bar{O}$ and CDF in all lepton channels [14] to the theoretical predictions from [7].

Atomic Energy (Russia), CAPES, CNPq and FAPERJ (Brazil), Departments of Atomic Energy and Science and Education (India), Colciencias (Colombia), CONACyT (Mexico), Ministry of Education and KOSEF (Korea), CONICET and UBACyT (Argentina), The Foundation for Fundamental Research on Matter (The Netherlands), PPARC (United Kingdom), Ministry of Education (Czech Republic), Natural Sciences and Engineering Research Council and West-Grid Project (Canada), BMBF (Germany), A.P. Sloan Foundation, Civilian Research and Development Foundation, Research Corporation, Texas Advanced Research Program, and the Alexander von Humboldt Foundation.

-
- [1] $D\bar{O}$ Collaboration, V. M. Abazov *et al.*, “Search for Neutral Higgs Bosons Decaying to tau pairs in $p\bar{p}$ Collisions at $\sqrt{s} = 1.96$ TeV”, *Phys. Rev. Lett.* **97**, 121802 (2006).
- [2] $D\bar{O}$ Collaboration, V. M. Abazov *et al.*, “First measurement of $\sigma(p\bar{p} \rightarrow Z) \times \text{Br}(Z \rightarrow \tau^+\tau^-)$ at $\sqrt{s} = 1.96$ TeV”, *Phys. Rev. D* **71**, 072004 (2005).
- [3] T. Andeen *et al.*, FERMILAB-TM-2365-E (2006).
- [4] T. Sjöstrand *et al.*, *Comput. Phys. Commun.* **135**, 238 (2001).
- [5] R. Brun and F. Carminati, CERN Program Library Long Writeup W5013, 1993 (unpublished).
- [6] $D\bar{O}$ Collaboration, B. Abbott *et al.*, “Measurement of the inclusive differential cross section for Z bosons as a function of transverse momentum in $p\bar{p}$ collisions at $\sqrt{s} = 1.8$ TeV”, *Phys. Rev. D* **56** (1997) 5558.
- [7] R. Hamberg, W.L. van Neerven and T. Matsuura, *Nucl. Phys. B* **359**, 343 (1991), and its errata in **644**, pg 403. Additional description of uncertainties can be found in hep-ph/0308087.
A.D. Martin, R.G. Roberts, W.J. Stirling, R.S. Thorne, *Phys.Lett. B* **604** (2004) 61-68.
- [8] W.-M. Yao *et al.*, *Journal of Physics G* **33**, 1 (2006).
- [9] C.F. Galea, “Tau Identification at $D\bar{O}$ ”, Proc. “Physics at LHC 2006, Cracow, Poland”, *Acta Physica Polonica B* (2007); Fermilab-Conf-06-462-E.
- [10] H.C. Fesefeldt, University of Aachen Technical Report PITHA 85-02 (1985).
- [11] C. Zeitnitz, A. Gabriel, “The GEANT-Calor Interface User’s Guide” ORNL, Oak Ridge (1996).
- [12] R. Hamberg, W.L. van Neerven and T. Matsuura, *Nucl. Phys. B* **359**, 343 (1991), and its errata in **644**, pg 403. Additional description of uncertainties can be found in hep-ph/0308087.
J. Pumplin *et al.*, *JHEP* **0207** (2002) 012.
D. Stump *et al.*, *JEP* **0310** (2003) 046.
- [13] S. Frixione, B.R. Webber, “Matching NLO QCD computations and parton shower simulations”, *JHEP* **06** (2002), 029.
- [14] CDF Collaboration, F. Abe *et al.*, “Measurement of $\sigma_B(W \rightarrow e\nu)$ and $\sigma_B(Z^0 \rightarrow e^+e^-)$ in $p\bar{p}$ Collisions at $\sqrt{s} = 1.8$ TeV”,

Phys. Rev. Lett. **76**, 3070 (1996).

CDF Collaboration, F. Abe *et al.*, “Measurement of Z^0 and Drell-Yan Production Cross Section Using Dimuons in $p\bar{p}$ Collisions at $\sqrt{s} = 1.8$ TeV”, Phys. Rev. D **59**, 052002 (1999).

DØ Collaboration, B. Abbott *et al.*, “Measurement of W and Z boson production cross sections (Run Ia)”, Phys. Rev. D **60** 052003 (1999).

CDF Collaboration, D. Acosta *et al.*, “First Measurements of Inclusive W and Z Cross Sections from Run II of the Fermilab Tevatron Collider”, Phys. Rev. Lett. **94**, 091803 (2005).

CDF Collaboration, A. Abulencia *et al.*, “Measurement of $\sigma(p\bar{p} \rightarrow Z) \cdot B(Z \rightarrow \tau\tau)$ in $p\bar{p}$ Collisions at $\sqrt{s} = 1.96$ TeV”, Phys. Rev. D **75**, 092004 (2007).